Effects of CuO and Fe_2O_3 Nanoparticles on Structural and Electrical Properties of Conjugated Polymer Blend Films

Bothaina M. Abed [1]
Mohammed G. Hammed [2]

[1] Basic Science Department, College of Medicine, University of Anbar, Ramadi, IRAQ
[2] Physics Department, College of Science, University of Anbar, Ramadi, IRAQ

Hybrid nanocomposite films were synthesized using a water-based casting method by blending polyvinyl alcohol (PVA) and polyaniline (PANI) in a 50:50 weight ratio. Copper oxide (CuO) and iron oxide (Fe_2O_3) nanoparticles, also in a 50:50 ratio, were incorporated at varying concentrations (0–10 wt.%) to enhance the properties of the films. X-ray diffraction (XRD) analysis confirmed that the polymer's semi-crystalline nature became more crystalline with increasing nanoparticle concentration. FTIR spectroscopy revealed significant changes in chemical bonding, indicating strong interactions between the polymers and nanoparticles. The FE-SEM analysis clearly demonstrates the influence of nanoparticle concentration on the surface morphology with uniform surface at low concentration and transform to rougher surface with agglomeration at high concentrations. Electrical conductivity measurements demonstrated improved charge carrier mobility, enhancing the films' overall conductivity. These findings suggest that the incorporation of CuO and Fe_2O_3 nanoparticles significantly improves the electrical properties of PVA/PANI composites, making them promising materials for electronic device applications.

Keywords: Polymer blends; Nanocomposites; Copper oxide; Nanoparticles
Received: 21 February 2025; **Revised:** 28 April 2025; **Accepted:** 4 May 2025

1. Introduction

Polymers have attracted considerable attention in device manufacturing because of their intrinsic properties, such as ease of fabrication, easy processability, light weight, flexibility, and high mechanical strength. Currently, combining two or more different polymers is a practical and easy method to create blends with unique physical properties. These polymer blends have attracted considerable attention because of their possible applications in the fields of desirable sizes, interfacial contacts, and thin film formation [1]. This process is an effective method for the preparation of a flexible polymeric matrix with a high degree of miscibility instead of new polymer synthesis [2,3]. Using polymers is a noticeable method in the manufacturing of semiconductors because polymer matrices enable processability due to solubility and control the growth and morphology of the nanoparticles [1]. There is growing scientific and technological attention for polymeric composites because of the high application range offered by these hybrid composites. This approach is gaining increasing attention because of the expected new uses of the produced materials, as well as their contribution to the basic sciences [4].

Organic semiconductors, originating from the transfer of π electrons from molecules to molecules, play an important role in the fundamental physical processes of living organisms. In general, polymers exhibit very poor electrical conductivity. Several polymers are electrically conductive or can be made conductive by doping with an electron donor or acceptor. Conducting polymers can be oxidized more easily and reversibly than conventional polymers. The charge transfer agents (dopants) affect this oxidation or reduction and in doing so convert an insulating polymer to a conducting polymer with near-metallic conductivity in metallic cases. Conducting polymers represent an important research area with diverse scientific problems of fundamental significance and potential for commercial application [5,6].

Polyvinyl alcohol (PVA) is a man-made thermoplastic polymer that dissolves in water [7]. Its chemical formula is $[CH_2CH(OH)]_n$. This cost-effective and easily manipulated polymer is typically produced commercially from the vinyl acetate monomer. PVA can undergo partial or complete hydrolysis, which may influence its final properties. The semi-crystalline nature of PVA is often attributed to the hydrogen bonding between its chains [8,9]. PVA offers strong optical transmission, corrosion resistance, thermal stability, and water solubility. Different PVA shapes have also shown promise in terms of biological and pharmacological characteristics. Membranes, sensors, coatings, fuel cells, adhesives, batteries, papermaking, textiles, nontoxic, biocompatible, sustainable, enhanced film and fiber formation, and biomedical frameworks are just a few of the industries where PVA has found use [10-13].

Polyaniline (PANI) is the most promising and most explored among conducting polymers, and it has high stability, high processability, tunable conducting, optical properties, easy synthesis, low price, elevated environmental stability, and good electrical properties

so it can be used as an electronic material. The conductivity of polyaniline is dependent upon the dopant concentration, and it gives metal-like conductivity only when the pH is less than 3 [14,15]. However, PANI has limited use owing to its poor solubility, mechanical properties, fusibility, and processability. To overcome these disadvantages, PANI is blended with water-soluble polymers such as polyvinyl alcohol (PVA) [16]. In recent years, numerous synthetic strategies have been utilized for the preparation of PANI/PVA films using PVA as a stabilizer [17]. Therefore, the produced blend (PVA/PANI) exhibits excellent properties for optical device applications. Moreover, the production and study of nanosized materials have attracted attention in research and technology because of their applications in optical and electronics manufacturing [18]. The consolidation of PVA, PANI, and metal nanocomposites will assist in the creation of novel materials that have improved optical, electrical, and structural properties [19,20].

Researchers have prepared nanocomposites using PVA and/or PANI with various nanofillers. The characteristics, geometry, and quantity of these nanofillers can influence the properties of these conductive polymer-based nanocomposites [21]. Metallic oxide nanoparticles alter the physical attributes of PVA and PANI based on their reinforcement efficiency. Typically, nanofillers comprising less than 5 wt.% are sufficient to improve the thermal and electrical conductivity, dimensional stability, strength, and modulus of the conjugated polymer nanocomposites [22]. A variety of nanofillers have been integrated into the PVA matrix to enhance the structural, optical, electrical, and mechanical properties of this versatile polymer [23].

The primary goal of this investigation is to find out how adding metal oxides, namely CuO and Fe_2O_3 nanoparticles, to the PVA:PANI blend structure affects the final morphology, structural characteristics, and electrical capabilities of the resultant nanocomposites.

2. Experiment Part

In this research, 30 ml of distilled water are used to dissolve 1 g of polyvinyl alcohol powder (produced by Alfa Chemistry Company, UK) with the chemical formula $[CH_2CH(OH)]_n$ and molecular weight 500 g/mol at a temperature of 60 °C using a magnetic stirrer for 6 h to ensure homogeneity of the solution. Next, the same amount of polyaniline (produced by Merck Company with the chemical formula C_6H_7N and molecular weight 67.09 g/mol was dissolved under the same conditions as before to obtain a homogeneous solution as well. After completing the preparation of the two solutions, they were mixed together in a 50:50 ratio using a magnetic stirrer to obtain homogeneity of the polyvinyl alcohol solution with the polyaniline solution.

Two types of nanoparticles were combined used as filler. Copper oxide (CuO) from Nanografi Co. of 99.5% purity. These nanoparticles have nearly spherical particle < 77 nm, and specific surface area greater than 20 m^2/g. The true density is around 6.5 g/cm^3. Elemental analysis indicates the presence of trace elements, including Fe at 0.008%, Ca at 0.003%, Mn at 0.003%, Mg at 0.007%, and Co at 0.006%. Iron oxide (Fe_2O_3) nanopowder from Nanografi Co. of 99.55%. These nanoparticles have spherical shapes of from 18 to 38 nm size. The specific surface area of these nanoparticles lies between 30 and 50 m^2/g. Elemental analysis revealed trace impurities, of Ca at 0.003%, Cr at 0.015%, Mn at 0.14%, Al at 0.05%, and SiO_2 at 0.091%. 1g of each powder was separately dispersed in 75 mL distilled water. A high-energy ultrasound device was used to ensure the prolonged suspension of these particles in the water. Subsequently, these suspended solutions of copper and iron oxide were incorporated into the previously prepared polymer blend at various concentrations (2, 4, 6, 8, and 10 wt.%). The final stage involves employing casting technology to create films from these materials on glass slides, with thicknesses ranging from 0.15 to 0.2 μm. These films were then subjected to various tests to determine their structural and electrical properties.

The nanocomposites films were analyzed using x-ray diffraction Rigaku Miniflex-II diffractometer with CuK_α radiation of wavelength 1.5406Å and angle (2θ) varying from 10° to 90°.

3. Results and Discussion

Figure (1) shows the XRD pattern of pure of (PVA+PANI) polymer blend films as a reference for other nanocomposites films to investigate the influence of CuO and Fe_2O_3 nanoparticles on the structure of these polymer blend composites. The XRD pattern of PVA appeared with a broad and weak hump located around a 20° diffraction angle corresponding to the (101) crystalline plane [24]. This semi-crystalline nature of PVA polymer and the results agreed with previous researchers in this field [25,26]. The semi-crystallinity of PVA is known to originate from the strong intermolecular interaction between its chains and efficient inter-molecular hydrogen bonding [27].

The XRD pattern of the PANI film shows several characteristic peaks attributed to different structural features of the PANI chains**.** The Peak at around 2θ = 11.49° (d_{hkl}= 7.69 Å) is associated with the inter-chain spacing in the PANI structure. In addition, the Peak at around 2θ = 23.35° (d_{hkl}= 3.80 Å) is attributed to the stacking of PANI chains in the lamellar structure. The intensity of this peak can indicate the degree of order in stacking PANI chains. While the peak at around 2θ = 35.46° (d_{hkl} = 2.53 Å) is associated with interactions between PANI chains in the inter-chain spacing [28].

The XRD pattern of PVA/PANI blend film reflects the combined structural features of both PVA and

PANI polymers. In this pattern, the broad peak corresponding to the PVA appeared around the diffraction angle of 2θ =20°. In addition, the XRD pattern displays the characteristic peaks of the PANI structure with higher intensities, enhancing the copolymer's crystallinity.

PVA contains hydroxyl (-OH) groups, while PANI has amine groups. When blended, these functional groups interact through hydrogen bonding, leading to better molecular alignment, enhancing the crystallinity of the copolymer. The degree of crystallinity that can affect the mechanical properties and thermal properties of the blend [29].

The inter-planar spacing values (d_{hkl}) between crystal planes were determined using the Bragg equation as presented in table (1) [30]

$$\lambda = 2\, d\, sin\theta \qquad (1)$$

where λ is the wavelength of the X-ray, n is the diffraction order, and θ refer to diffraction angle. Scherrer's principle was used to calculate the crystallite size values (D) using the formula [31]:

$$D\ (nm) = \frac{0.94\,\lambda}{\beta.\cos\theta} \qquad (2)$$

were β is the breadth of the diffraction line in radians. Table (1) lists the diffraction peaks and their parameters

The small crystallite size corresponded to the PVA of 5.4 nm, while more significant for the PANI structure of 44.1 nm along the preferred orientation around 23.5° diffraction angle and enhanced after blending the polymers.

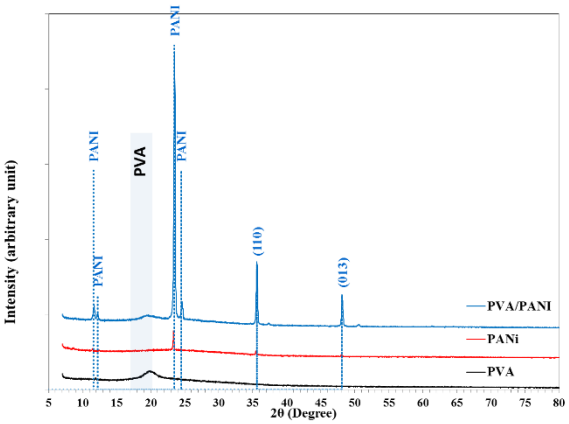

Fig. (1) XRD patterns of PVA, PANI, and (PVA+PANI) blend

Figure (2) shows that the XRD patterns of PVA/PANI:CuO-Fe_2O_3 NPs with varying concentrations of the NPs illustrate the structural variation of the polymer matrix as both metal oxides are incorporated. The broad diffraction hump corresponds to the PVA, and the diffraction peaks associated with PANI remain visible in all samples. Several distinct peaks emerge, confirming the presence of hematite structure and the observation of additional diffraction peaks corresponding to CuO. Their intensity increases with the increase in the two NPs' content.

Table (1) XRD parameters of PVA, PANI, and (PVA+PANI) blend

Sample	2θ (Deg.)	FWHM (Deg.)	d_{hkl} (Å)	C.S (nm)	Phase
PVA	19.957	1.500	4.4454	5.4	PVA
PANI	11.495	0.189	7.6917	42.2	PANI
	23.354	0.184	3.8059	44.1	PANI
	35.460	0.186	2.5294	44.8	PANI
	48.008	0.178	1.8936	48.9	PANI
Blend	11.692	0.174	7.5625	45.9	PANI
	12.211	0.174	7.2426	45.9	PANI
	19.670	1.630	4.5097	4.9	PVA
	23.518	0.175	3.7798	46.5	PANI
	24.629	0.180	3.6117	45.1	PANI
	35.615	0.163	2.5188	51.3	PANI
	48.131	0.154	1.8890	56.6	PANI

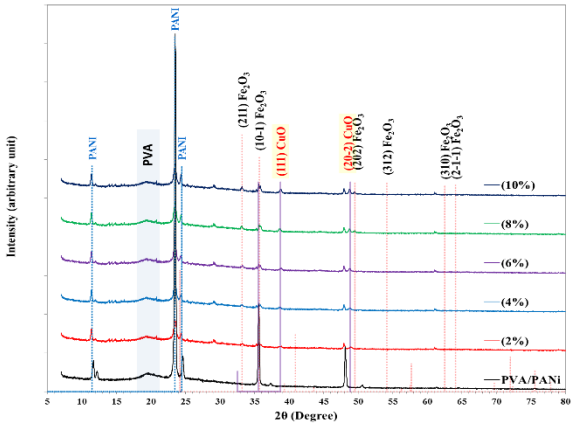

Fig. (2) XRD patterns of the blend+CuO+Fe_2O_3 nanocomposite films

The presence of both Fe_2O_3 and CuO indicates the formation of a hybrid inorganic-organic nanocomposite, where the interplay between the metal oxides and polymer significantly influences the structural properties.

The combined presence of Fe_2O_3 and CuO within the PVA/PANI matrix is estimated to enhance the functional properties. The increase in crystallinity due to metal oxide incorporation may improve the electrical conductivity and optical behavior of the nanocomposites.

The FTIR spectra within the range of 400 to 4000 cm^{-1} for the PVA and PVA:PANI polymer blend are shown in Fig. (3). The FTIR spectrum of the PVA displays the characteristic bands corresponding to the functional groups of this polymer. The stretching vibration of the hydroxyl group (-OH) was found around 3400 cm^{-1}. The stretching C-H bands are found at 2920 and 2852 cm^{-1}, corresponding to asymmetric and symmetric vibration modes in alkyl groups [32].

The O-H bending vibration appeared at 1736 cm^{-1}. The C=O bending vibration was at 1659 cm^{-1}, a prominent characteristic of PVP [33]. The -CH_2 symmetric bending mode was observed at 1440 cm^{-1} [34]. The band around 1103 cm^{-1} is associated with C-O vibration further confirm the presence of characteristic PVA functionalities [35].

After blending with PANI in a 50:50 ratio, noticeable spectral changes occur. The broad O–H band near 3400 cm^{-1} is significantly reduced in intensity, which may be attributed to partial replacement by N–H stretching of PANI, whose absorption band overlaps in this region. The band corresponding to C-O was shifted to 1093 cm^{-1}, suggests some interaction between the hydroxyl groups in PVA and the amine groups in PANI. The increased intensity of this Peak compared to pure PVA shows the interactions between the two polymers. New peaks observed at 1654 and 1424 cm^{-1} are attributed to C=C quinoid/benzenoid stretching and C–N stretching modes of PANI [36]. Table (3) summarizes the FTIR bands in PVA and PVA:PANI blend samples.

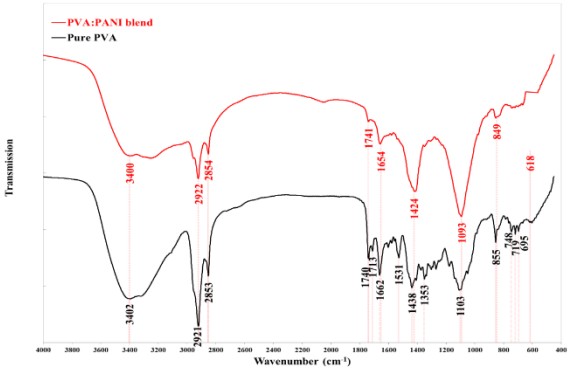

Fig. (3) FTIR spectra of PVA and PVA/PANI blend

Table (3) Bands corresponding to bonds and the oscillation pattern of PVA and PVA+PANI polymer blends

Band assignments Pure	Wavenumber (cm^{-1})	
	PVA	PVA/PANI
-OH (Stretching/vibration)	3400	3400
C-H (stretching)	2920	2923
	2852	2852
C=O Stretching	1736	1736
C=O vibration	1659	1654
-CH_2 symmetric bending	1440	1424
C-O Stretching	1103	1093
C-H bending	604-855	614-853

Figure (4) illustrates the transmission FTIR patterns of (PVA-PANI) blend composed with CuO:Fe_2O_3 NPs at various concentrations (2%, 4%, 6%, 8%, and 10%). Variations in peak characteristics are observed based on the nanoparticle concentrations [37]. The 2921 and 2852 cm^{-1} dual bands correspond to C-H stretch vibration bonds, which are common to both PVA and PANI polymers, bands appear attenuated in the nanocomposite spectra after the addition of CuO–Fe_2O_3 hybrid nanoparticles, which can be explained by restricted chain mobility caused by physical rather than chemically interactions of the oxide nanoparticles with the polymer chains [38]. The suppression of vibrational modes and a slight shift in their location such as C–H and O–H, can be attributed to electrostatic interaction between the positively charged ions of the metal oxide and the ionic pairs of the polymers, where the oxide particles restrict the motion of the polymer chains [39]. Additional bands appeared at 618 and 490 cm^{-1} correspond to metal oxides (Fe-O). Table (4) lists the FTIR bands of PVA:CuO/Fe_2O_3:PANI films at different concentrations [40].

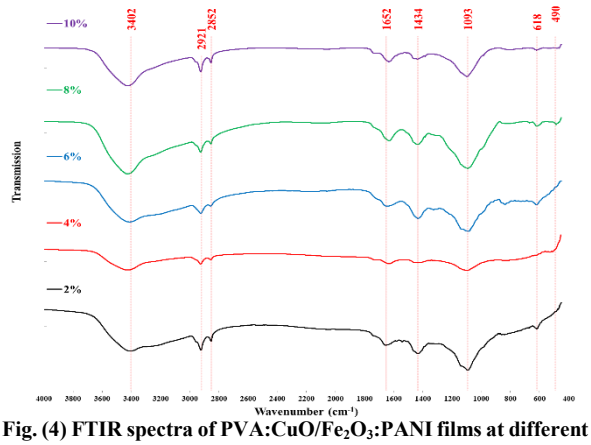

Fig. (4) FTIR spectra of PVA:CuO/Fe_2O_3:PANI films at different concentrations

Table (4) FTIR bands of PVA:CuO/Fe_2O_3:PANI films at different concentrations

Band Assignments Pure	Wavenumber (cm^{-1})				
	2%	4%	6%	8%	10%
-OH Stretching	3402	3426	3427	3412	3426
C-H Stretching	2921	2924	2924	2923	2923
	2852	2854	2855	2855	2853
C=C Stretching	1652	1634	1629	1647	1633
C-N Stretching	1434	1433	1440	1432	1434
C-O Stretching	1093	1092	1100	1086	1094
Fe-O	618	616	618	619	619
	490	490	490	490	490

Figure (5) displays the surface morphology of conductive polymer PANI:PVA blend films and their nanocomposites reinforced with an equal ratio of CuO and Fe_2O_3 at varying concentrations, through FE-SEM images at two magnifications. The pure PVA:PANI blend exhibits a smooth surface with no observable cracks, indicating excellent film-forming properties and compatibility between the PVA and PANI components. Such surface topography may influence the material's electrical and mechanical properties [41]. Upon the addition of 2 wt.% of CuO–Fe_2O_3, the surface remains relatively uniform, with the emergence of fine granular features with sizes ranging from approximately 22 to 35 nm, indicates good dispersion and interaction of the nanoparticles within the polymer matrix. Increasing the concentration to 4 wt.% leads to a rougher surface with larger particles (27–38 nm), although dispersion remains acceptable. At 6 wt.% adding, the surface becomes rougher and more pronounced aggregates, indicating reduced dispersion efficiency, as a result of the polymer matrix is becoming saturated with nanoparticles. At 8 wt.%, more aggregated domains and the possible formation of phase-separated regions within the matrix. Finally, at

the highest concentration of 10 wt.%, the surface becomes highly irregular, marked by the appearance of large clusters up to 138 nm and even cracks. The evident agglomeration and phase separation at this stage indicate poor nanoparticle dispersion and weak interaction with the host polymer.

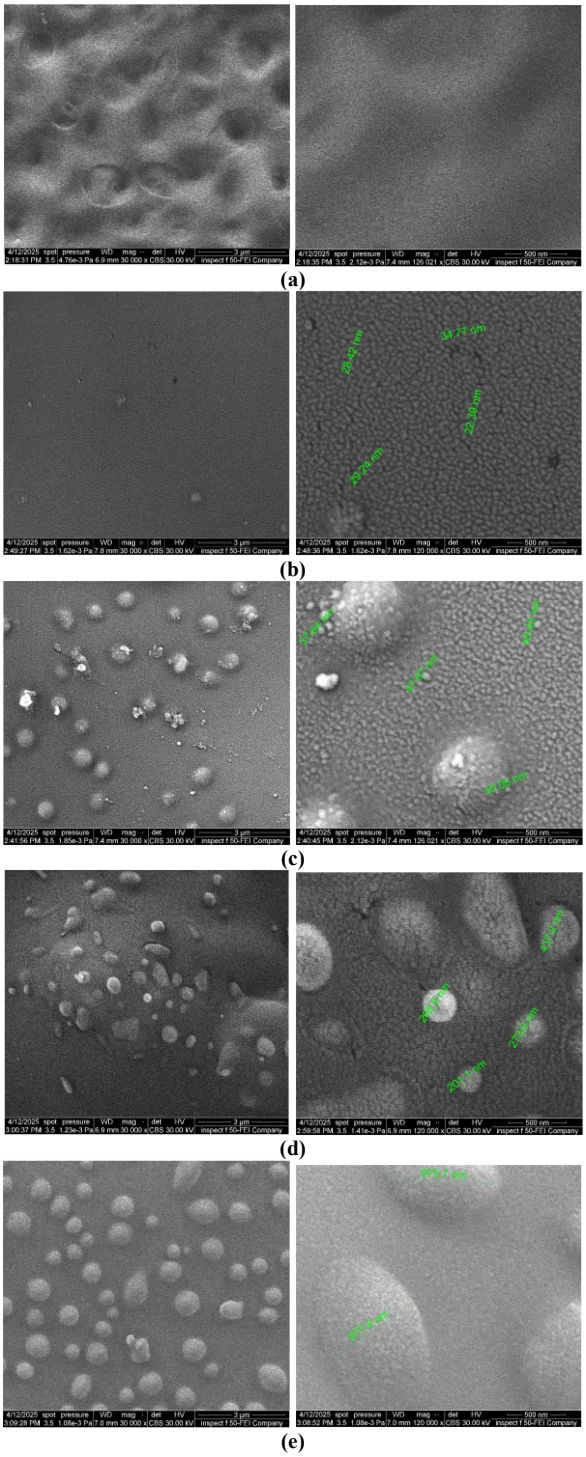

(a) (b) (c) (d) (e)

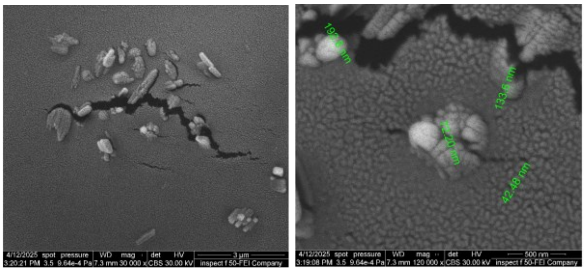

(f)

Fig. (5) FE-SEM images at two magnifications for PVA/PANI blend (a) and the reinforced samples with CuO:Fe_2O_3 hybrid nanoparticle at (b) 2, (c) 4, (d) 6, (e) 8, and (f) 10 wt.%

Figure (6) displays the energy-dispersive X-ray (EDX) spectroscopy of the PANI:PVA blend films and their nanocomposites at various CuO and Fe_2O_3 concentrations. The EDX spectrum of the pure PVA:PANI film shows dominant peaks for C, N, O, which are characteristic elements of the both polymers. Two additional emissions appear around 1.7 keV and 2.2 keV, corresponding to Si in glass substrate and Au corresponding to the gold coating applied to the samples prior to FE-SEM. Upon incorporation of 2 wt.% CuO–Fe_2O_3 nanoparticles, additional peaks corresponding to Cu and Fe appear, indicating successful integration of the metal ions into the blend. These peaks are of relatively low intensity at this ratio. Increases the added up to 10% increases the intensities of Cu and Fe peaks. Table (5) lists the elemental analysis of the samples at the different concentrations.

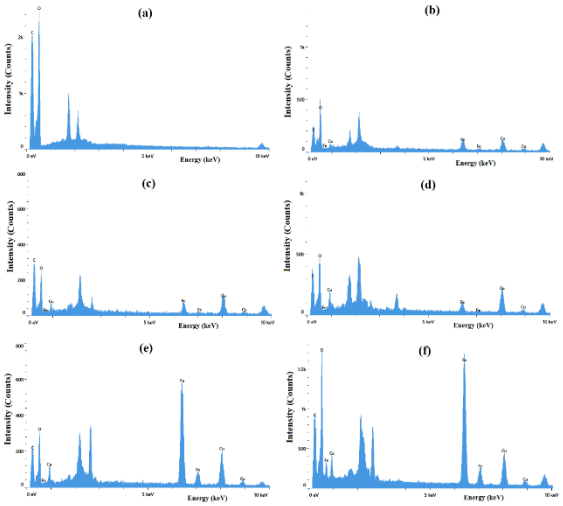

Fig. (6) EDX analysis for PVA/PANI blend (a) and the reinforced samples with CuO:Fe_2O_3 hybrid nanoparticle at (b) 2, (c) 4, (d) 6, (e) 8, and (f) 10 wt.%

The impact of adding copper and iron oxides on the electrical characteristics of the PVA:PANI blend were investigated by Hall effect measurement, a method for determining the nature, concentration, and mobility of charge carriers. Adding varying concentrations of CuO and Fe_2O_3 NPs to PVA: PANI blends with various ratios results in negative R_H across all concentrations,

suggesting that n-type conductivity is maintained. These oxides act as electron donors, increasing the number of free electrons in the material and thus increasing the conductivity, which is consistent with the research [42]. In addition, there is a general increase in the concentration of charge carriers (N_H) with an increase in the percentage of CuO and Fe_2O_3. This indicates that the addition of these oxides contributes to the increase in the number of free electrons in these films. On the contrary, a decrease in the mobility value was observed is some samples with increasing NP concentration. This reduction in mobility occurs due to the increased scattering of electrons caused by lattice defects introduced by the addition of NPs. Therefore, metal oxides play a significant role in altering the electrical properties of the nanocomposite films by increasing the concentration of free electrons while simultaneously reducing their mobility. The electrical conductivity remained relatively constant, even though the charge carrier concentration increased and the mobility decreased. This indicates that the effects of the higher charge carrier concentration were largely reduced in mobility.

Table (5) EDX analysis results of PVA:PANI/CuO:Fe_2O_3 films at different NPs concentrations

Sample	Element	Atomic %	Weight %
0	C	48.4	41.6
	O	51.6	58.4
2%	C	48.2	34.2
	O	45.7	43.2
	Fe	1.1	3.8
	Cu	5	18.8
4%	C	55.7	41.7
	O	39.3	39.1
	Fe	1.3	4.6
	Cu	3.7	14.6
6%	C	42.1	29.7
	O	51.9	48.8
	Fe	2.5	8.1
	Cu	3.6	13.4
8%	C	44.7	27.8
	O	43.2	35.8
	Fe	8.9	25.7
	Cu	3.2	10.6
10%	C	49	27.4
	O	33.4	24.9
	Fe	12.4	32.1
	Cu	5.3	15.6

Table (6) Hall effect parameters of PVA, PANI, PVA:PANI, and their composites with CuO and Fe_2O_3 NPs

Sample	R_H (cm^3/C)	N_H (cm^{-3})	σ $(\Omega.cm)^{-1}$	μ ($cm^2/V.s$)	Type
0	-0.0100	6.25E+17	0.00746	0.00007	N
2%	-0.0199	3.14E+17	0.01200	0.00024	N
4%	-0.0109	5.75E+17	0.01170	0.00013	N
6%	-0.0067	9.28E+17	0.01350	0.00009	N
8%	-0.0022	2.87E+18	0.01195	0.00003	N
10%	-0.0050	1.26E+18	0.01500	0.00007	N

The electrical conductivity (σ) of the PVA:PANI/CuO:Fe_2O_3 nanocomposites films with the weight percentage of the nanoparticle additives was shown in Fig. (7). The combination of copper oxide and iron oxide can be explained as creating a combined effect, as both contribute to improved conductivity. Copper oxide acts as a semiconductor material, while iron oxide promotes reactions within the material, increasing the transfer of electrical charges.

This phenomenon explains that introducing conductive additives such as Fe_2O_3 and CuO NPs into a polymer blend creates a continuous network, improving conductivity. The observed fluctuations in conductivity suggest interactions between the additives and the polymers blend matrix, potentially resulting from alterations in microstructure. These observations align with research on polymer nanocomposite films, which demonstrates that optimal additive dispersion leads to enhanced conductivity at specific concentrations [43,44].

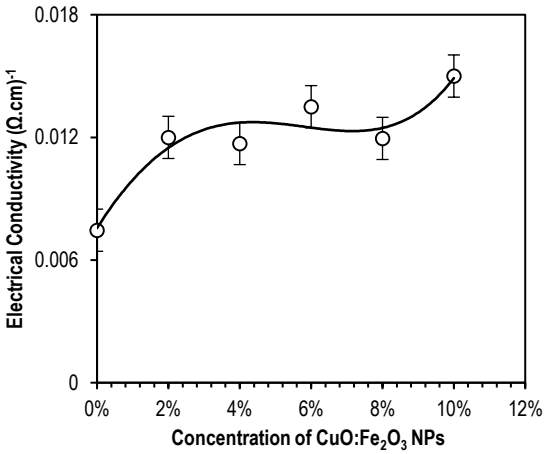

Fig. (7) DC conductivity of PVA:PANI/CuO:Fe_2O_3 nanocomposites at different concentrations of CuO:Fe_2O_3 nanoparticles

4. Conclusions

This study demonstrated that incorporating CuO and Fe_2O_3 nanoparticles into PVA/PANI blend enhances their structural, optical, and electrical properties. XRD confirmed improved crystallinity, while FTIR indicated strong polymer-nanoparticle interactions. The FE-SEM analysis clearly demonstrates the influence of nanoparticle concentration on the surface morphology. While lower concentrations promote good dispersion and relatively uniform surfaces, higher concentrations lead to increased agglomeration and rougher surface. The EDX spectra confirm the presence and gradual enrichment of Cu and Fe in the polymer blend with increasing nanoparticle content. Optical analysis showed increased absorbance and a reduced energy gap. Electrical measurements highlighted enhanced conductivity and carrier concentration, with CuO at 4 wt.% shifting with N-type conductivity. These

improvements make PVA/PANI nanocomposites suitable for applications in flexible electronics, sensors, and optoelectronic devices.

References

[1] M.G. Hammed and A.A. Hassan, "Enhancement of the Structural and Optical Properties of (PVA-PANI) Polymer Blend by Addition of CuI Nanoparticles", IOP Conf. Ser.: Mater. Sci. Eng., 928 (2020) 072157.

[2] M.A. Morsi et al., "Preparation, structural analysis, morphological investigation and electrical properties of gold nanoparticles filled polyvinyl alcohol/carboxymethyl cellulose blend", *J. Mater. Res. Technol.*, 8 (2019) 5996–6010.

[3] I.S. Elashmawi and A.A. Al-Muntaser, "Influence of Co_3O_4 nanoparticles on the optical, and electrical properties of CMC/PAM polymer: combined FTIR/DFT study", *J. Inorg. Organomet. Polym. Mater.*, 31 (2021) 2682–90.

[4] A. Abou Elfadl et al., "Influence of α-Fe_2O_3, CuO and GO 2D nano-fillers on the structure, physical properties and antifungal activity of Na-CMC--PAAm blend", *Sci. Rep.*, 13 (2023) 12358.

[5] S. Srilalitha, K. Jayaveera and S. Madhvendhra, "The effect of dopant, temperature and band gap on conductivity of conducting polymers", *Int. J. Innov. Res. Sci. Eng. Technol.*, 2 (2013) 2694–2696.

[6] K. Namsheer and C.S. Rout, "Conducting polymers: a comprehensive review on recent advances in synthesis, properties and applications", *RSC Adv.*, 11 (2021) 5659–5697.

[7] A. Kausar, "Innovations in poly (vinyl alcohol) derived nanomaterials", *Adv. Mater. Sci.*, 20 (2020) 5–22.

[8] C.F. Mok et al., "Adsorption of dyes using poly (vinyl alcohol) (PVA) and PVA-based polymer composite adsorbents: a review", *J. Polym. Enviro.*, 28 (2020) 775–793.

[9] T. Siddaiah et al., "Structural, optical and thermal characterizations of PVA/MAA: EA polyblend films", *Mater. Res.*, 21 (2018) e20170987.

[10] S.K. Murad and S.H. Kadhim, "Synthesis, Characterization and Electrical Conductivity of Poly Vinyl Alcohol Graft Adipic Acid and Application as Sensors", *Int. J. Pharmaceut. Res.*, 12 (2020).

[11] L. Das et al., "Synthesis of hybrid hydrogel nano-polymer composite using Graphene oxide, Chitosan and PVA and its application in waste water treatment", *Enviro. Technol. Innov.*, 18 (2020) 100664.

[12] R.G. Kadhim, M.A. Habeeb and Q.M. Jebur, "Study the Structure, electrical and optical properties for (PVA-CMC-CuO) Bio nano composites", *J. Chem. Pharmaceut. Sci.*, 10 (2017) 1120–1127.

[13] J. Bhadra and N. Al-Thani, "Advances in blends preparation based on electrically conducting polymer", *Emerg. Mater.*, 2 (2019) 67–77.

[14] A.G. Enad, E.T. Abdullah and M.G. Hamed, "Study the electrical properties of carbon nanotubes/polyaniline nanocomposites", *J. Phys. Conf. Ser.*, 1178 (2019) 12032.

[15] M.M. Abdelhamied et al., "Synthesis and optical properties of PVA/PANI/Ag nanocomposite films", *J. Mater. Sci.: Mater. in Electron.*, 31 (2020) 22629–22641.

[16] J. Wang et al., "Facile synthesis of multi-functional elastic polyaniline/polyvinyl alcohol composite gels by a solution assembly method", *RSC Adv.*, 10 (2020) 22019–22026.

[17] Z. Renkler, I. Cruz Maya and V. Guarino, "Optimization of Polyvinyl Alcohol-Based Electrospun Fibers with Bioactive or Electroconductive Phases for Tissue-Engineered Scaffolds", *Fibers*, 11 (2023) 85.

[18] M. Beygisangchin et al., "Preparations, properties, and applications of polyaniline and polyaniline thin films—A review", *Polymers*, 13 (2021) 2003.

[19] M.M. Abdelhamied et al., "Oxygen ion induced variations in the structural and Linear/Nonlinear optical properties of the PVA/PANI/Ag nanocomposite film", *Inorg. Chem. Commun.*, 133 (2021) 108926.

[20] H. Donya et al., "Micro-structure and optical spectroscopy of PVA/iron oxide polymer nanocomposites", *J. Mater. Res. Technol.*, 9 (2020) 9189–9194.

[21] A. Samzadeh-Kermani, M. Mirzaee and M. Ghaffari-Moghaddam, "Polyvinyl alcohol/polyaniline/ZnO nanocomposite: synthesis, characterization and bactericidal property", *Adv. Biol. Chem.*, 6 (2016) 1–11.

[22] K.M.A. Saron et al., "Controlling the dielectric and optical properties of polyvinyl alcohol/polyethylene glycol blends by adding copper oxide nanoparticles for application in energy storage devices", *J. Sol-Gel Sci. Technol.*, 109 (2024) 757–772.

[23] M. Aslam, M.A. Kalyar and Z.A. Raza, "Polyvinyl alcohol: A review of research status and use of polyvinyl alcohol based nanocomposites", *Polym. Eng. Sci.*, 58 (2018) 2119–2132.

[24] M. Das and D. Sarkar, "Development of room temperature ethanol sensor from polypyrrole (PPy) embedded in polyvinyl alcohol (PVA) matrix", *Polym. Bull.*, 75 (2018) 3109–3125.

[25] S.B. Aziz et al., "Polymer Blending as a Novel Approach for Tuning the SPR Peaks of Silver Nanoparticles", *Polymers*, 9 (2017) 486.

[26] Z.A. Alrowaili et al., "Significant Enhanced Optical Parameters of PVA-Y_2O_3 Polymer Nanocomposite Films", *J. Inorg. Organomet. Polym. Mater.*, 31 (2021) 3101–3110.

[27] X. Wei et al., "Intermolecular interactions between starch and polyvinyl alcohol for improving mechanical properties of starch-based straws", *Int. J. Biol. Macromole.*, 239 (2023) 124211.

[28] J. Liu et al., "Constructing sandwich-like polyaniline/graphene oxide composites with tunable conjugation length toward enhanced microwave absorption", *Organ. Electron.*, 63 (2018) 175–183.

[29] K. Sangam Naidu and S. Palaniappan, "Formation of PANI-PVA salt via H-bonding between PVA and PANI: Aqueous coating for electrostatic discharge, sensor and corrosion applications", *Sens. Int.*, 1 (2020) 100006.

[30] M.C. Morris, **"Standard X-ray Diffraction Powder Patterns"**, US Department of Commerce, National Institute of Standards and Technology (1978).

[31] M. De Graef and M.E. McHenry, **"Structure of Materials: An Introduction to Crystallography, Diffraction and Symmetry"**, Cambridge University Press (2012).

[32] BB.H. Stuart, **"Infrared Spectroscopy: Fundamentals and Applications"**, Wiley (2004).

[33] V. Kumar et al., **"Radiation Effects in Polymeric Materials"**, Springer International Publishing (2019).
[34] G. Gerlach and K.F. Arndt, **"Hydrogel Sensors and Actuators: Engineering and Technology"**, Springer (Berlin, 2009).
[35] C.M. Hussain, **"Handbook of Nanomaterials for Industrial Applications"**, Elsevier (2018).
[36] Q.A. Acton, **"Advances in Nanotechnology Research and Application"**, Scholarly Editions (2012).
[37] T. Kobayashi and T. Yamazaki, "Fe_2O_3/CuO Hybrid Nanostructures as Electrode Materials for Glucose Detection", *Anal. Bioanal. Chem. Res.*, 121 (2020) 8–9.
[38] A. Kharazmi et al., "Structural, optical, opto-thermal and thermal properties of ZnS-PVA nanofluids synthesized through a radiolytic approach", *Beilstein J. Nanotech.*, 6 (2015) 529–536.
[39] N.T. Nagaraj et al., "Polyaniline Ingrained Copper Oxide (PANI/CuO) Nanocomposites for Effective Electromagnetic Interference Shielding and Their Sensitive Detection of Dopamine", *Anal. Bioanal. Electrochem.*, 16(7) (2024) 628-642.
[40] B.P. Swain, **"Nanostructured Materials and their Applications"**, Springer Nature (Singapore, 2020).
[41] J. Bhadra et al., "Polyaniline/polyvinyl alcohol blends: Effect of sulfonic acid dopants on microstructural, optical, thermal and electrical properties", *Synth. Metals*, 191 (2014) 126–134.
[42] A. Alnagar et al., "Exploring the structural, optical and electrical characteristics of PVA/PANi blends", *Opt. Mater.*, 139 (2023) 113771.
[43] S. Sharma et al., "Recent Trends and Developments in Conducting Polymer Nanocomposites for Multifunctional Applications", *Polymers*, 13 (2021) 2898.
[44] S.-Y. Lee et al., "Nanocellulose reinforced PVA composite films: Effects of acid treatment and filler loading", *Fibers Polym.*, 10 (2009) 77–82.

Table (2) XRD parameters of the blend+CuO+Fe_2O_3 nanocomposite films

Sample	2θ (Deg.)	FWHM (Deg.)	d_{hkl} (Å)	C.S (nm)	Phase	hkl
2%	11.312	0.202	7.8159	39.5	PANI	-
	23.578	0.293	3.7703	27.7	PANI	-
	24.520	0.304	3.6275	26.7	PANI	-
	33.272	0.330	2.6907	25.1	Fe_2O_3	(211)
	38.765	0.453	2.3210	18.6	Mono. CuO	(111)
4%	11.314	0.260	7.8142	30.7	PANI	-
	23.534	0.323	3.7772	25.1	PANI	-
	33.318	0.297	2.6870	27.9	Fe_2O_3	(211)
	35.492	0.243	2.5272	34.3	Fe_2O_3	(10-1)
	38.741	0.407	2.3225	20.7	Mono. CuO	(111)
	48.862	0.397	1.8624	22.0	Mono. CuO	(20-2)
6%	11.317	0.317	7.8126	25.2	PANI	-
	23.548	0.343	3.7750	23.7	PANI	-
	33.242	0.267	2.6930	31.0	Fe_2O_3	(211)
	35.611	0.219	2.5191	38.2	Fe2O3	(10-1)
	38.739	0.367	2.3226	23.0	Mono. CuO	(111)
	48.786	0.357	1.8652	24.4	Mono. CuO	(20-2)
8%	11.281	0.371	7.8376	21.5	PANI	-
	23.549	0.368	3.7748	22.0	PANI	-
	33.152	0.241	2.7001	34.4	Fe2O3	(211)
	35.593	0.197	2.5203	42.4	Fe2O3	(10-1)
	38.705	0.330	2.3245	25.5	Mono. CuO	(111)
	48.746	0.322	1.8666	27.1	Mono. CuO	(20-2)
	49.620	0.240	1.8358	36.5	Fe2O3	(202)
10%	11.339	0.332	7.7970	24.1	PANI	-
	23.515	0.339	3.7802	23.9	PANI	-
	33.194	0.217	2.6968	38.3	Fe2O3	(211)
	35.857	0.196	2.5024	42.6	Fe2O3	(10-1)
	38.770	0.297	2.3208	28.4	Mono. CuO	(111)
	48.871	0.289	1.8621	30.1	Mono. CuO	(20-2)
	49.620	0.230	1.8358	38.1	Fe2O3	(202)

